Figure 6.8. Three-wavelength color composite HV-polarization radar image of Kilauea volcano and Ka'u desert, Hawai'i. Red tones correspond to C-band (5.7 cm), green to L-band (24 cm), and blue to P-band (68 cm) echoes. (Calibrated data courtesy T. Farr, JPL, and P. Mouginis-Mark, University of Hawaii).

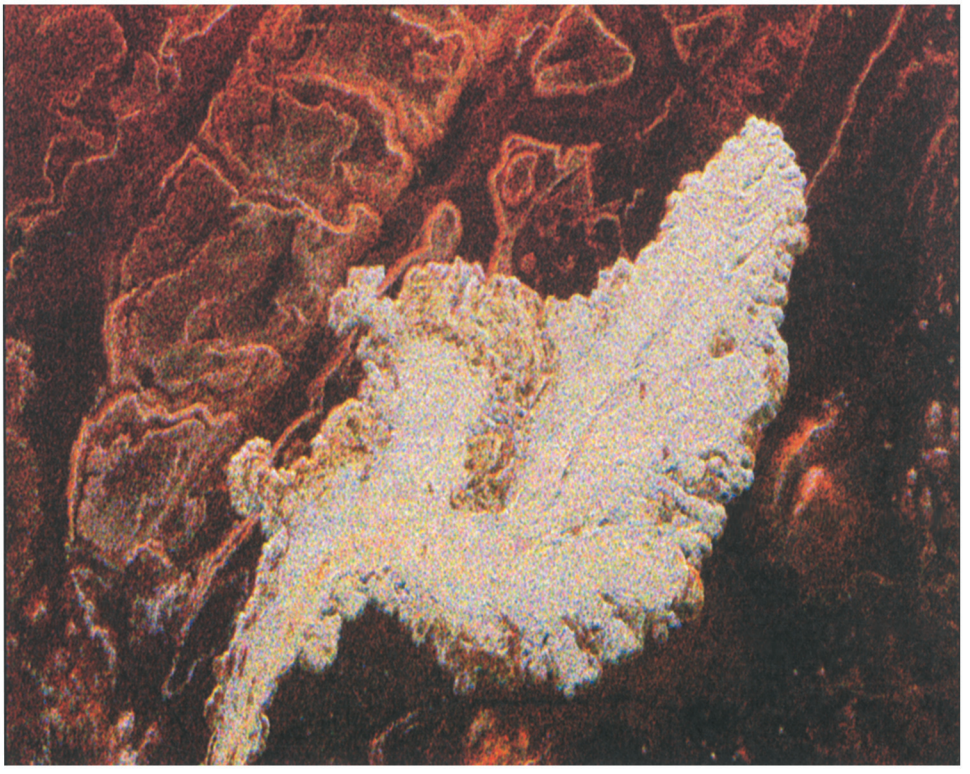

Figure 6.21. Three-wavelength color composite, HV-polarization radar image of SP flow. Red tones correspond to C-band (5.7 cm), green to L-band (24 cm), and blue to P-band (68 cm) echoes. Note the subtle trace of a central channel (high C-band returns, lower L- and P-band echoes) in the proximal region of the flow. Backscatter from the main lobe of the flow is largely saturated at all three wavelengths (courtesy NASA/JPL).

These plates are available for download in color from www.cambridge.org/9780521583084

Figure 7.16. AIRSAR three-wavelength (red = 5.7 cm, green = 24 cm, blu = 68 cm wavelength) HH-polarization image of sand dune field (top center) in Death Valley, CA. Image width 8 km. Note the bright glints from radar-facing dune slopes near the top of the image (courtesy NASA/JPL).

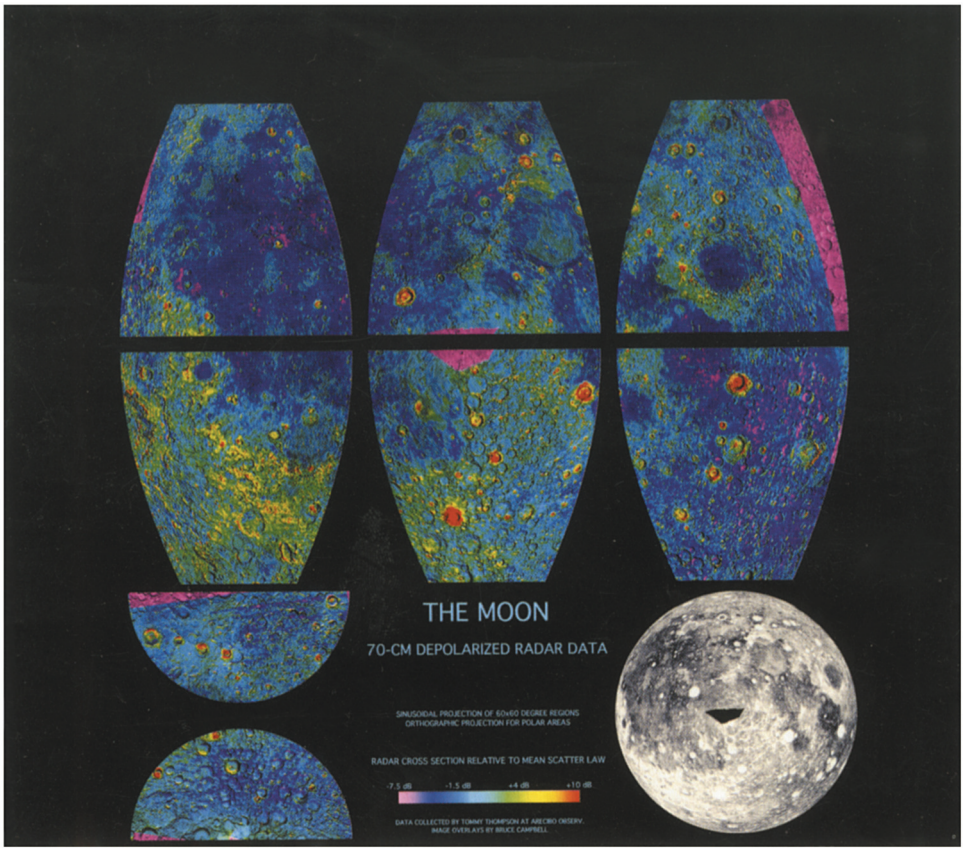

Figure 8.4. Like-polarized circular-polarization lunar radar images at 70 cm wavelength (data from Thompson [1987]), overlain on a USGS shaded-relief map. Data presented as sinusoidal-projection maps of 60°×60° areas centered on –60°, 0°, and 60° E longitude. Polar areas shown in orthographic projection.

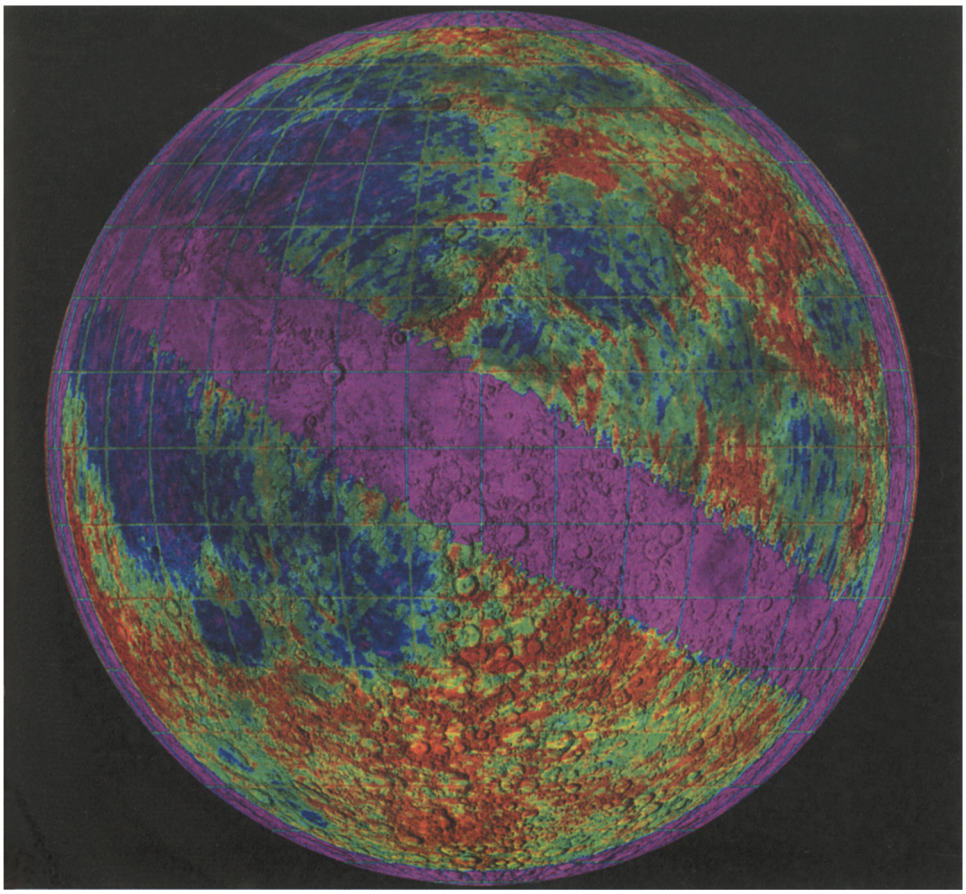

Figure 8.5. Cross-polarized circular-polarization lunar radar image at 7.5 m wavelength (data from Thompson [1974]), overlain on a USGS shaded-relief map. Orthographic projection.

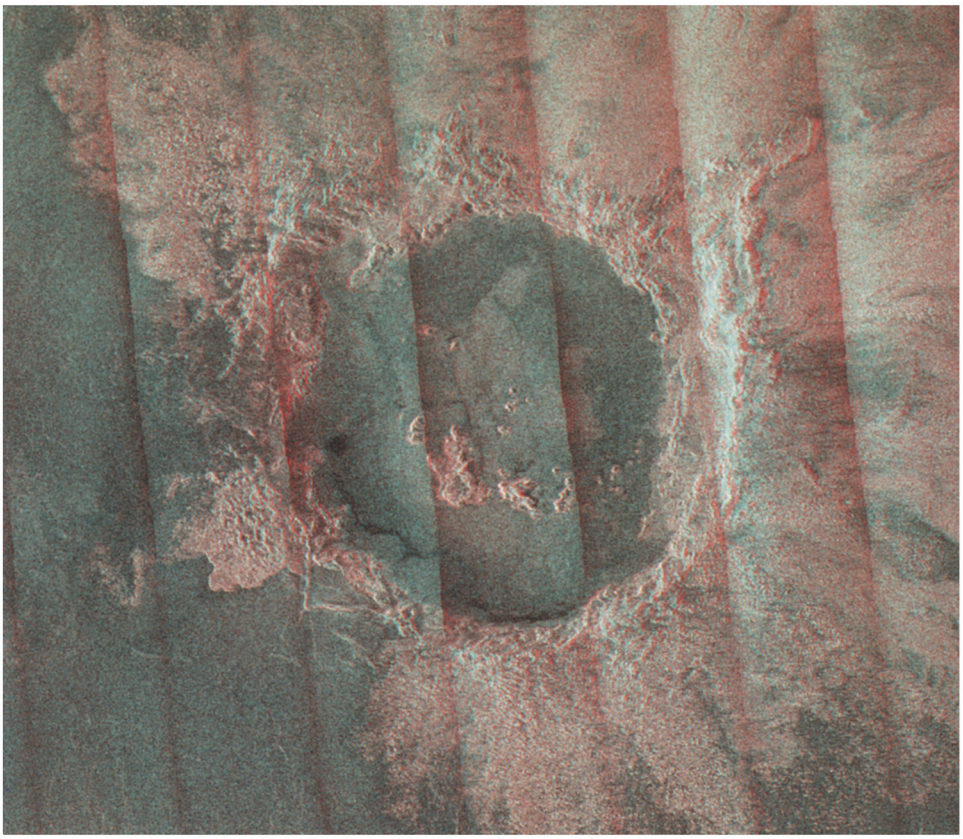

Figure 9.7. Radar "anaglyph" of Markham crater (72 km diameter). The Magellan cycle-1 left-looking data are shown in the red channel, while cycle-3 left-looking stereo data are shown in the green and blue channels. This image may be viewed in stereo with red–blue glasses. The "window-blind" effect is due to uncorrected beam pattern effects in the cycle-3 image data.

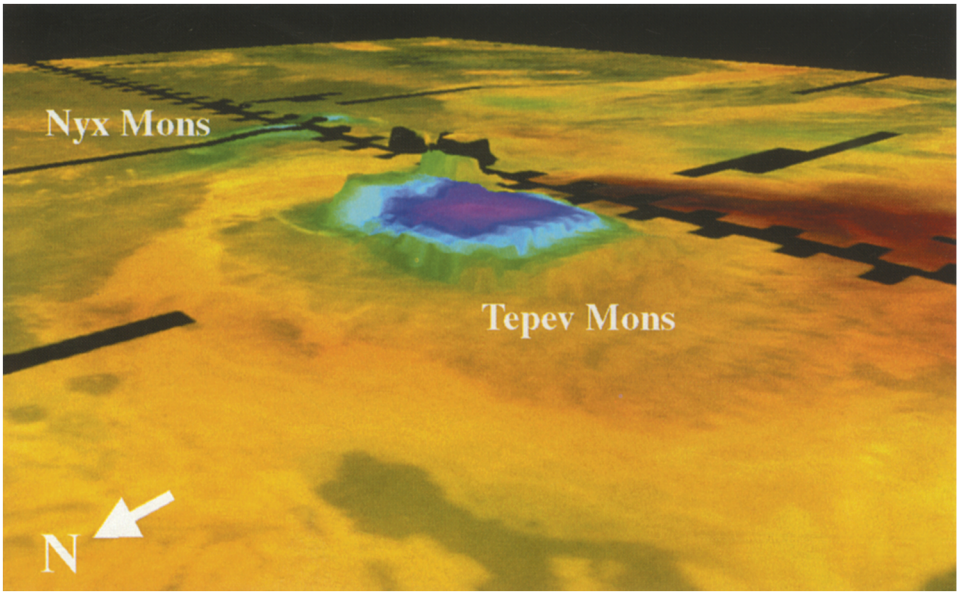

Figure 9.14. Horizontally polarized emissivity data for Bell Regio, overlain on a three-dimensional view of the topography. High emissivity is noted by red, low emissivity as purple and blue. Note that only the highest parts of Tepev and Nyx Montes have markedly low emissivity (higher reflectivity).

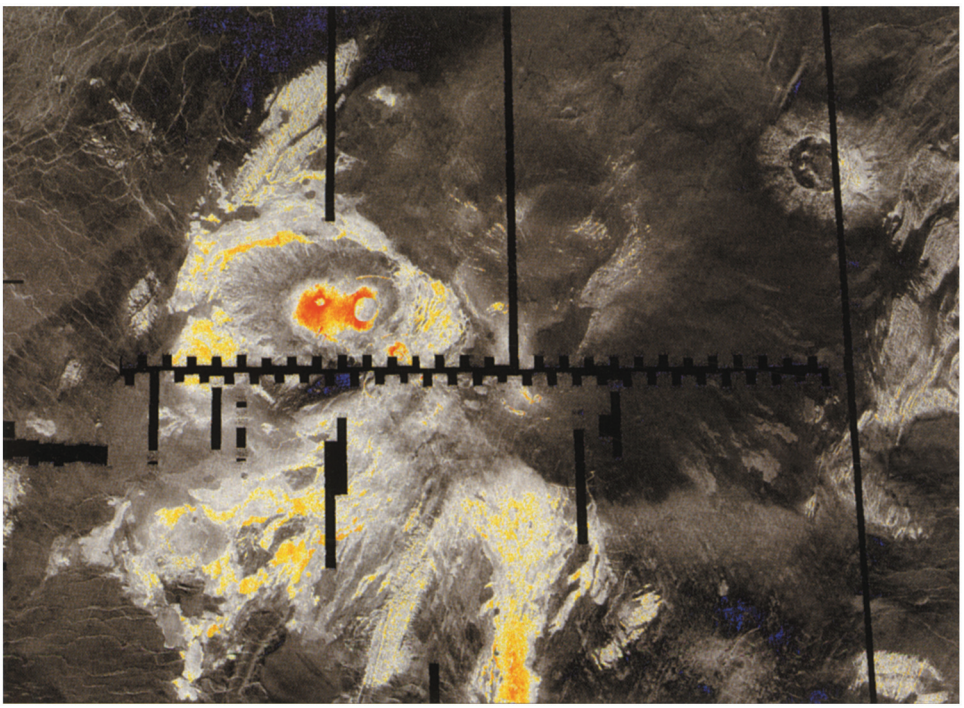

Figure 9.16. Color-coded Magellan image of Bell Regio, showing very rough surfaces (> –10 to –3 dB) in shades of yellow through red, and very low backscatter regions (< –25 dB) in blue.

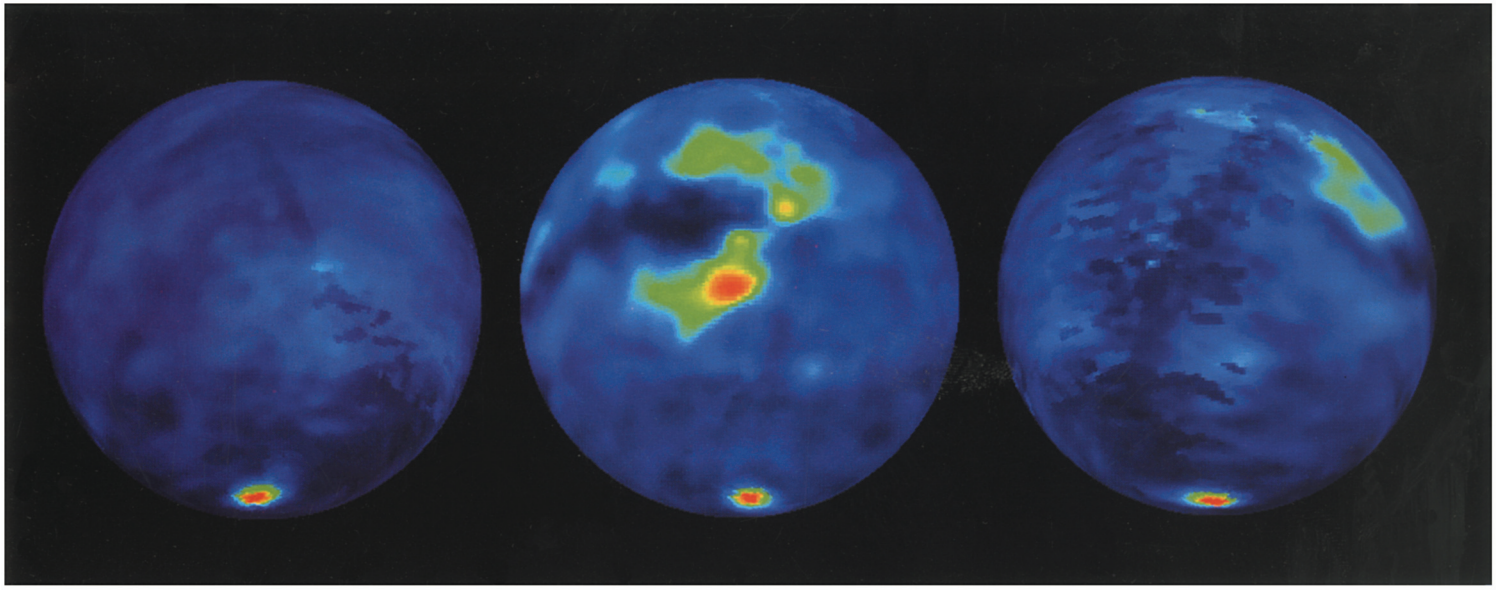

Figure 9.28. VLA radar maps of Mars (courtesy B. Butler, NRAO). These three images show the planet at sub-radar longitudes of 0° W, 120° W, and 240° W; the sub-radar latitude is –24°. The bright return at the bottom of each image is due to the south polar cap. The radar-dark "Stealth" area is visible to the left of the bright Tharsis region in the center image.

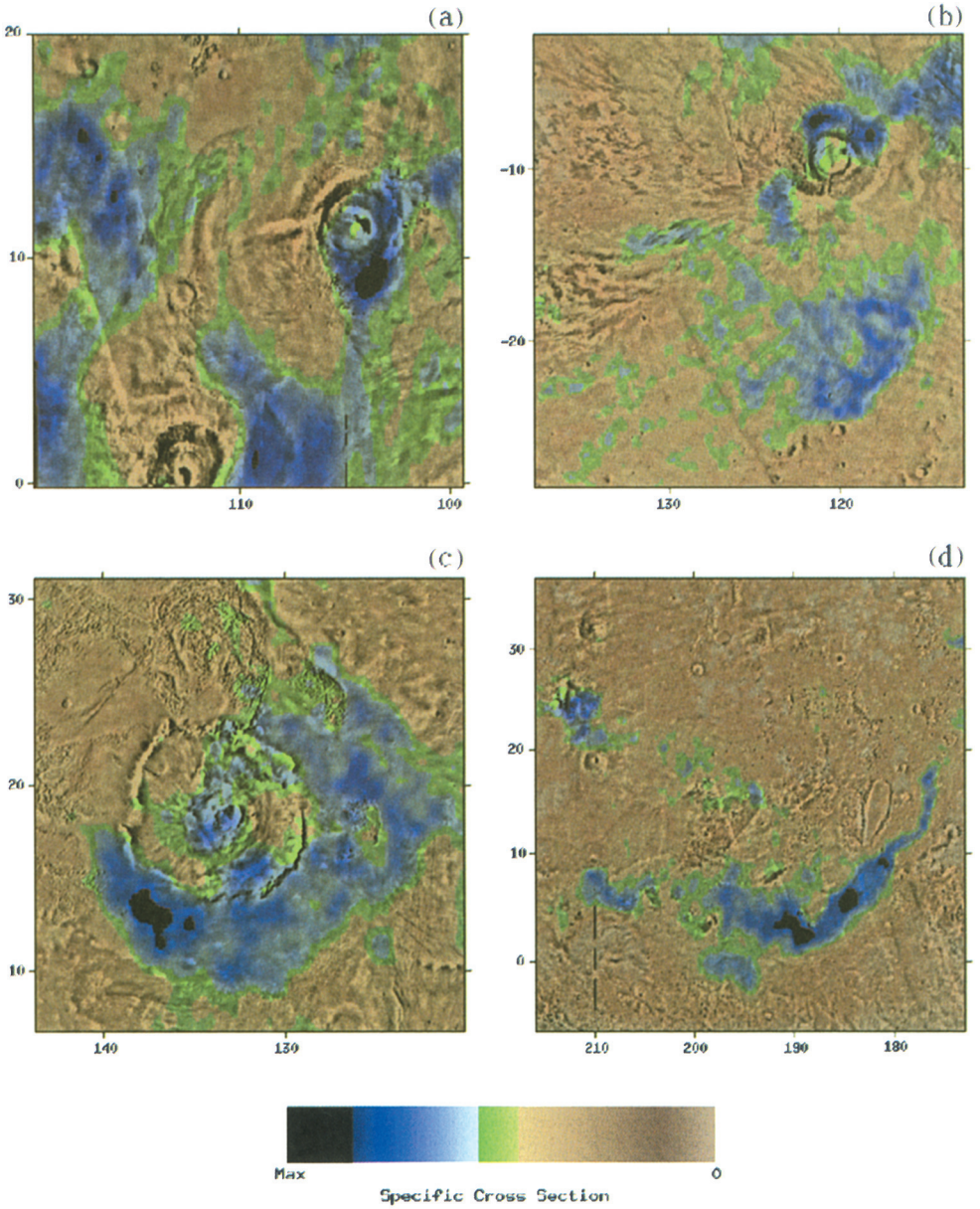

Figure 9.29. Color plot of co-polarized circular (LL) backscatter coefficient, overlain on a shaded relief map, for four Mars regions (courtesy J. Harmon, Arecibo Observatory). (a) Northern Tharsis; (b) Southern Tharsis and Daedalia Planum; (c) Olympus Mons; (d) Elysium region. Note that higher radar backscatter is indicated by blue to black tones.